

Variations and gradients between methane seep and off-seep microbial communities in a submarine canyon system in the Northeast Pacific

Susie Cummings¹, Lila M. Ardor Bellucci², Sarah Seabrook³, Nicole A. Raineault⁴, Kerry L. McPhail⁵ and Andrew R. Thurber^{1,2}

- Department of Microbiology, College of Science, Oregon State University, Corvallis, OR, United States of America
- ² College of Earth, Ocean, and Atmospheric Sciences, Oregon State University, Corvallis, OR, United States of America
- ³ National Institute of Water and Atmospheric Research, Wellington, New Zealand
- ⁴ University of South Florida, St. Petersburg, FL, United States of America
- ⁵ College of Pharmacy, Oregon State University, Corvallis, OR, United States of America

ABSTRACT

Methane seeps are highly abundant marine habitats that contribute sources of chemosynthetic primary production to marine ecosystems. Seeps also factor into the global budget of methane, a potent greenhouse gas. Because of these factors, methane seeps influence not only local ocean ecology, but also biogeochemical cycles on a greater scale. Methane seeps host specialized microbial communities that vary significantly based on geography, seep gross morphology, biogeochemistry, and a diversity of other ecological factors including cross-domain species interactions. In this study, we collected sediment cores from six seep and non-seep locations from Grays and Quinault Canyons (46–47°N) off Washington State, USA, as well as one non-seep site off the coast of Oregon, USA (45°N) to quantify the scale of seep influence on biodiversity within marine habitats. These samples were profiled using 16S rRNA gene sequencing. Predicted gene functions were generated using the program PICRUSt2, and the community composition and predicted functions were compared among samples. The microbial communities at seeps varied by seep morphology and habitat, whereas the microbial communities at non-seep sites varied by water depth. Microbial community composition and predicted gene function clearly transitioned from on-seep to off-seep in samples collected from transects moving away from seeps, with a clear ecotone and high diversity where methane-fueled habitats transition into the non-seep deep sea. Our work demonstrates the microbial and metabolic sphere of influence that extends outwards from methane seep habitats.

Subjects Ecology, Ecosystem Science, Marine Biology, Microbiology, Biological Oceanography **Keywords** Methane seeps, Microbial ecology, Biogeochemistry, Deep sea, 16S rRNA gene analysis, Predictive gene function, Ocean sediment, Northeast pacific ocean

Submitted 20 January 2023 Accepted 2 March 2023 Published 28 March 2023

Corresponding author Susie Cummings, cumminsu@oregonstate.edu

Academic editor Angelo Bernardino

Additional Information and Declarations can be found on page 16

DOI 10.7717/peerj.15119

© Copyright 2023 Cummings et al.

Distributed under Creative Commons CC-BY 4.0

OPEN ACCESS

INTRODUCTION

Oceanic methane seeps are an important component of the global methane budget, which requires careful consideration as methane is a potent greenhouse gas (Kvenvolden, 1988; Reeburgh, 2007; Ruppel & Kessler, 2017). Specifically, methane seeps are sites of significant biological handling of methane, as the anaerobic oxidation of methane (AOM) performed by microbes at seeps captures an estimated 80-90% of subsurface methane before it reaches the water column (Reeburgh, 2007; Luff & Wallmann, 2003). The central microbial processes at methane seeps are the paired reactions of methane oxidation and sulfate reduction, carried out primarily by a partnership between archaeal anaerobic methane oxidizers (ANME) and sulfate-reducing bacteria (SRB) (Boetius et al., 2000; Orphan et al., 2002). Seeps are also occupied by endemic fauna that form unique habitats, most commonly sulfidic polychaete worm beds, Bathymodiolin mussel beds, Vesicomyid clam beds, and Lamellibrachia tube worm bushes (Levin et al., 2003; Sahling et al., 2003; Guillon et al., 2017). Methane seeps and their associated microbes also provide sources of food for deep-sea creatures, ranging from seep-endemic species to mobile, commercially important species (Levin et al., 2016; Seabrook, De Leo & Thurber, 2019; Turner et al., 2020; Thurber et al., 2012). For this reason, it is important to track the "sphere of influence" of methane seeps, which can also be indicated within the microbial communities in sediment adjacent to the areas that are visibly impacted by seepage (Levin et al., 2016).

Seeps vary in their microbial community composition, including in their distributions of the different ANME and SRB clades. ANME-1 and ANME-2 are more abundant globally than ANME-3. ANME-2 generally predominates at cold seep sites below 20 °C (Ruff et al., 2015; Wegener et al., 2016), whereas ANME-1 is tolerant of a broader range of temperatures and can even exist at hydrothermal vents (Vigneron et al., 2013; Wegener et al., 2016). ANME-1 is also more abundant at seeps with high fluid flow and anoxic conditions, such as the carbonate chimneys of the Black Sea (Ruff et al., 2015; Wegener et al., 2016; Treude et al., 2007). ANME-3 appears to be more common at colder temperatures, especially at high latitudes (e.g., the Arctic and Antarctic), but can also appear at cold seeps of greater depth and at mud volcanoes (Niemann et al., 2009; Bhattarai et al., 2017; Ruff et al., 2019). The clades of sulfate-reducing bacteria as partners of ANME also vary between different seep sites but are most commonly Desulfobacterales of the clades SEEP-SRB1 through -SRB4 (Wegener et al., 2016; Petro et al., 2019; Waite et al., 2020). Though ANME at seeps frequently pair with SRB partners, some clades can carry out methane oxidation without a partner, especially ANME-3 (Vigneron et al., 2013; Bhattarai et al., 2017). Seep macrofauna also have distinctive microbial communities associated with them, often as symbiotes within their tissues. The activities of macrofauna additionally affect the sediment-based microbial communities by changing physical parameters such as the penetration of oxygen and sulfide via bioturbation and bioirrigation (Wallmann et al., 1997; Thurber et al., 2013; Felden et al., 2014; Guillon et al., 2017).

The above variations in methane seep microbial community composition also suggest a corresponding diversity of gene functions at seeps. In addition to methane and sulfur cycling, another important area of focus is nitrogen cycling. Certain ANME are capable of nitrogen fixation and perform high rates of nitrogen fixation at seeps, with rates dependent on methane concentration (Dekas et al., 2014; Dekas et al., 2018; Kapili et al., 2020). Additionally, the clade ANME-2d (also known as Candidatus Methanoperedens spp.) can perform its methane oxidation with nitrate as an electron acceptor rather than sulfate (Haroon et al., 2013; Berger et al., 2021). In a broader context, deep sea microbes within and beyond seeps play important roles in nitrogen cycling. The rates of nitrogen fixation, nitrification, denitrification, and anammox in the deep sea are higher than previously expected, a discrepancy which may be explained by microbial metabolism (Pachiadaki et al., 2017; Wang et al., 2017; Suter et al., 2021). Along with nitrogen, trace metals play an important role in deep sea microbial metabolisms. Some clades of anaerobic methane oxidizers can directly use iron and manganese as alternate electron acceptors to sulfate, notably ANME-2d (Beal, House & Orphan, 2009; Leu et al., 2020). Iron, nickel, cobalt, molybdenum, and tungsten are also integral to enzymes for central metabolism, methanotrophy, and nitrogen cycling in ANME and sulfate-reducing bacteria (Glass & Orphan, 2012; Glass et al., 2014). Since the mining of heavy metals in the deep sea is of increasing industrial interest (Levin & Sibuet, 2012; Gillard et al., 2019), it is correspondingly important to examine how microbes use these metals in their metabolisms.

The Cascadia Margin, located in the Pacific Ocean off the coast of the northwestern United States, has been an area of interest for methane seep research since the earliest discoveries of methane seeps (*Suess et al., 1985*). Methane seepage is prolific in this area, and has been occurring for thousands of years (*Joseph et al., 2013*). Recent surveys of the Cascadia Margin with single-beam and multibeam sonar have detected 3,481 methane bubble plumes, corresponding to 1,300 subsurface sources of methane fueling these seep sites (*Merle et al., 2021*). The seep habitats of the Cascadia Margin vary in geological structure, as well as macrofaunal and microbial community composition; including carbonate rock platforms, methane hydrate fields, soft sulfidic sediment, microbial mats, Vesicomyid clam beds, and Lamellibrachia tube worm beds (*Boetius & Suess, 2004*; *Seabrook et al., 2018*).

Here, six seep and non-seep sites of the Cascadia Margin were sampled to assess the biological and chemical gradients from off-seep to on-seep. For this study, we quantify the shift of microbial community and metabolic transitions between non-seep and seep sites, including based on sediment geochemistry. Two of the seep sites, Dagorlad Seep and Emyn Muil Seep, were sampled *via* comprehensive transects. These two seeps have very different gross morphology, which we interpret as an indication of the age of each seep. The stage of microbial succession is discussed in this context.

MATERIALS & METHODS

Study sites and sampling

Samples were collected as part of the *E/V Nautilus* expedition NA121 in September and October 2020, which focused on Grays and Quinault Canyons (46–47°N) off the coast of Washington State, USA (Table 1, Fig. 1). Sediment push cores (internal diameter 6.4 cm) were collected from various seep and non-seep sites using ROV Hercules. For two seeps,

Table 1 Site descriptions.						
Site	Latitude, Longitude	Depth (m)	Cores collected	Description		
Quinault 500 m	47.253, -125.035	500	2	Non-seep; rocky carbonate platforms >50 m away from active seepage		
Westmarch Seep	47.173, -125.145	1310	2	Seep vesicomyid clam bed with dark reduced sediment and polychaete worms		
Quinault Canyon, ridge	47.081, -125.058	1040	1	Non-seep; \sim 100 m deep canyon with glass sponges on ridge		
Quinault Canyon, bottom	47.083, -125.060	1120	2	Non-seep; \sim 100 m deep canyon (same as above); canyon base with fish and starfish present		
Emyn Muil Seep	46.783, -125.262	1070	5	Seep site with thick rocky carbonate platforms; also featured areas of Calyptogena clam beds, dark reduced sediment, and small microbial mats		
Dagorlad Seep	47.057, -125.028	1010	6	Seep site with extensive (\sim 50 m wide) microbial mat and soft sediment; vesicomyid clams on periphery of mat		
OOI Regional Cabled Array	44.515, -125.390	2900	2	Slope Base site (PN1A); non-seep site near southern Hydrate Ridge		

named "Dagorlad" and "Emyn Muil," a transect-based sampling scheme was used to assess biogeochemical gradients from "off-seep" to "on-seep." This was achieved by marking the location of active methane seepage, and sampling in a line: 150 m from seep, 50 m from seep, 5 m from seep, and on-seep.

To contrast with a background sample, we also included two sediment cores from the Slope Base site of the Ocean Observatories Initiative Regional Cabled Array at 2,900 m water depth (44.5152°N, -125.3898° W). This site was located 300 km south of the other samples and was included to compare a deeper non-seep site of the same geographical region. These samples were collected by *ROV Jason* during routine maintenance of the OOI site.

Cores were extruded shipboard and sectioned into one cm-deep samples of sediment, ranging from surface (0 cm) to 10 cm deep in the core, with the exterior discarded to prevent sediment smearing from impacting the measured microbial community. These samples were frozen at $-80~^{\circ}\text{C}$ for microbiological analysis and porewater was extracted using Rhizons (0.15 μ m pore size) inserted into cores at two cm intervals, often from a core collected adjacent to the one used for microbiology (if not the same core used for microbiology). Porewater was frozen at $-20~^{\circ}\text{C}$ (for major ions) or preserved in 0.05 M zinc acetate and refrigerated at 4 $^{\circ}\text{C}$ (for hydrogen sulfide). Sediment samples for methane analysis were collected in three cm sediment fractions using a sub-core, and were preserved by mixing with two mL of 5M NaOH and refrigerating upside-down at 4 $^{\circ}\text{C}$.

Methane, sulfide, and sulfate measurements

Ions were analyzed on an Integrion Ion Chromatograph at Oregon State University using an IonPac CS16-4 μ m, 4 \times 250 mm column. Methane samples were analyzed on a Picarro G2131-i Cavity Ring Down Spectrometer coupled to a Small Sample Injection Module at Oregon State University. Stabilized sulfide samples were quantified on a Shimadzu

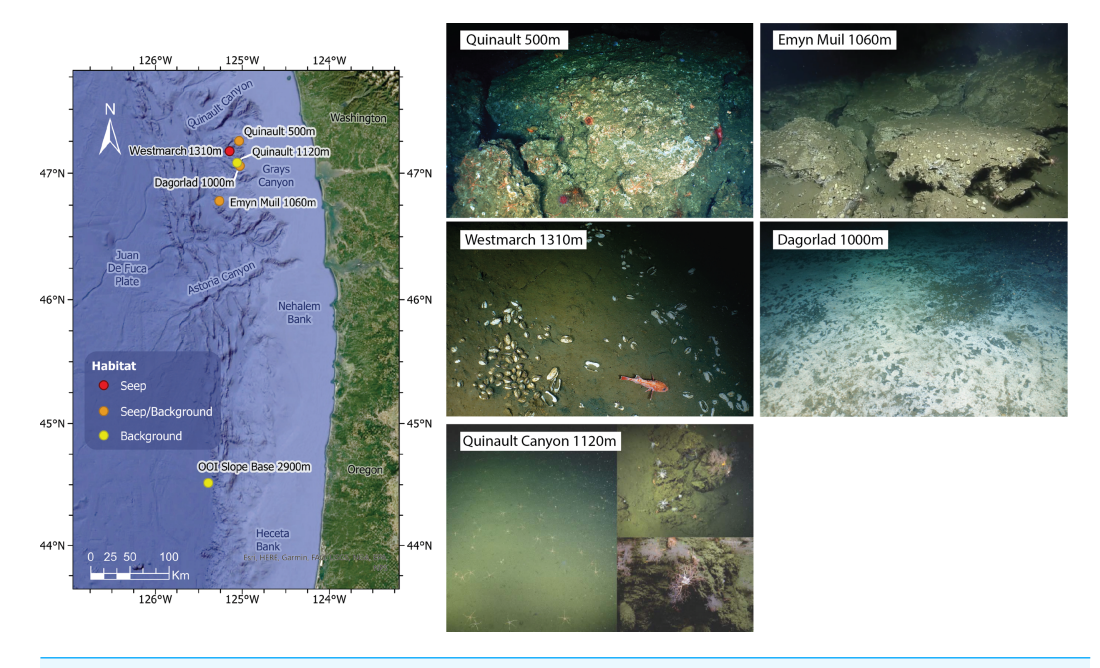


Figure 1 Map and seep imagery. Map of sampling sites and ROV imagery from each site. Quinault 500 m was an active seep site at 500 m depth, but samples were only taken from 180 m and 50 m off-seep due to uncoreable rock on-seep. Westmarch Seep was a small seep at 1,310 m depth indicated by a vesicomyid clam bed. Quinault Canyon was a non-seep canyon site at 1,120 m depth (at base) with images shown from the canyon floor (left) and canyon walls (right). Emyn Muil was a seep at 1,060 m depth with extensive, deep carbonate platforms. Dagorlad Seep was a seep at 1,000 m depth with a large (>50 m wide) white and grey microbial mat. OOI Slope Base was located at the 2,900 m depth Oregon Slope Base Site of the Ocean Observatories Initiative's Regional Cabled Array; ROV imagery for this site was not available.

Full-size DOI: 10.7717/peerj.15119/fig-1

UV-1201S spectrophotometer at 670 nm following Cline's methylene blue method (*Cline*, 1969).

DNA extraction and sequencing

Frozen sediment samples were extracted for DNA using the QIAgen PowerSoil kit, starting with 0.25—0.50 g of sediment and following the standard kit protocol. After DNA extraction, samples were sequenced following the Earth Microbiome protocol, wherein the V4 16S rRNA region is amplified using the improved F515/R806 primers (*Walters et al.*, 2015), as detailed in a previous paper (*Seabrook et al.*, 2018). Sequencing was carried out at the Oregon State University Center for Qualitative Life Sciences on the Illumina MiSeq platform, with 250-bp paired-end reads. Sequencing depth for these samples was on average 48,000 reads per sample and ranged from 1,000 to 210,000 reads.

The full set of 16S rRNA gene data was deposited in the SRA archive and is available under Bioproject PRJNA718843.

Data analysis and statistics

Bioinformatics of the 16S rRNA analysis was carried out using a QIIME2 (v2021.2) pipeline, using DADA2 and the SILVA 16S database v138.1 (*Bolyen et al.*, 2019; full pipeline provided in Data S1). We employed the PICRUSt2 program, which provides predictive gene family

profiles and functions inferred from the 16S genes present (*Douglas et al.*, 2020). Statistics and figure generation, based on the outputs of the QIIME2 and PICRUSt2 analyses, were carried out in RStudio with the packages phyloseq (*McMurdie & Holmes*, 2013), vegan (*Oksanen et al.*, 2020), ANCOM-BC (*Lin & Peddada*, 2020), and microbiome (*Lahti et al.*, 2017). Additional figures were generated *via* SigmaPlot 14.0 (Systat Software Inc.).

For statistical analysis, the amplicon sequence variant (ASV) table output from QIIME2 was used, as well as the KEGG pathway/KO number table output from PICRUSt2. For both data sets, samples with sequencing depth below 4,000 reads were filtered out. Data were then rarefied to 4,000 and Chao1 richness metrics were calculated. Shannon alpha-diversity metrics were also calculated but found to show similar patterns to Chao1 (Table S1). Nonmetric multidimensional scaling (NMDS) plots were generated using Bray-Curtis distance. The PICRUSt2 output was used to curate a database of genes (Table S2) for iron and metal transport as well as sulfur, nitrogen, and methane metabolism. This database was used to focus our analysis on particular genes and processes of interest for seep systems.

RESULTS

Microbial community composition

Analysis of the V4 region of the 16S rRNA gene microbial communities identified a total of 72,649 ASVs. 5,492 of these ASVs were singletons. When samples were grouped as either seep-associated (microbial mat, clam bed, ampharetid bed) or non-seep (5 m off-seep, 50 m off-seep, 150 m off-seep, or OOI non-seep sediment), there were differences between the microbial communities (Fig. 2A; PERMANOVA P < 0.001, pseudo-F = 25.43, DF = 212). There were 11,631 ASVs that appeared only at seep sites, including 3,539 Archaeal ASVs. At the dominant taxa level, there were also clear and gross community differences between the seep sites (Emyn Muil, Dagorlad, and Westmarch Seeps; Fig. 3) and non-seep sites. We employed an ANCOM (via the ANCOMBC R package) analysis to pinpoint microbial families that were statistically different between non-seep and seep sites (Fig. 4, Table S3). The bacterial families Scalinduaceae, Woeseiaceae, and NB1-j were significantly more abundant in non-seep sites vs. seep sites. In non-seep sites, Scalinduaceae made up on average $4.3 \pm 3.4\%$ of the microbial community, and Woeseiaceae and NB1-j made up $5.1 \pm 4.3\%$ and $4.9 \pm 2.7\%$, respectively. On the other hand, all seep sites had Sulfurovaceae, Desulfobacteraceae, and Sulfurimonadaceae as prominent families. At seep sites, Sulfurovaceae made up on average $5.0 \pm 4.9\%$ of the microbial community, and Desulfobacteraceae and Sulfurimonadaceae made up $2.8 \pm 2.6\%$ and $3.5 \pm 4.6\%$ respectively. Despite these moderate means, certain taxa were very prominent in individual samples. For example, in one microbial mat core from Dagorlad Seep, Sulfurimonadaceae made up 23.1% of the total microbial community at the surface, and Sulfurovaceae made up 24.6% of the total microbial community at three cm depth. Individual seep sites also showed variation in particular bacterial families present. Desulfosarcinaceae, the family containing SEEP-SRB1, was present at all seep sites (8.1 \pm 5.3% of the microbial community) but was particularly abundant at Emyn Muil Seep (11.9 \pm 5.4%). Desulfocapsaceae, the family containing SEEP-SRB4, was present in small numbers at all seep sites (1.8 \pm 2.4%), but

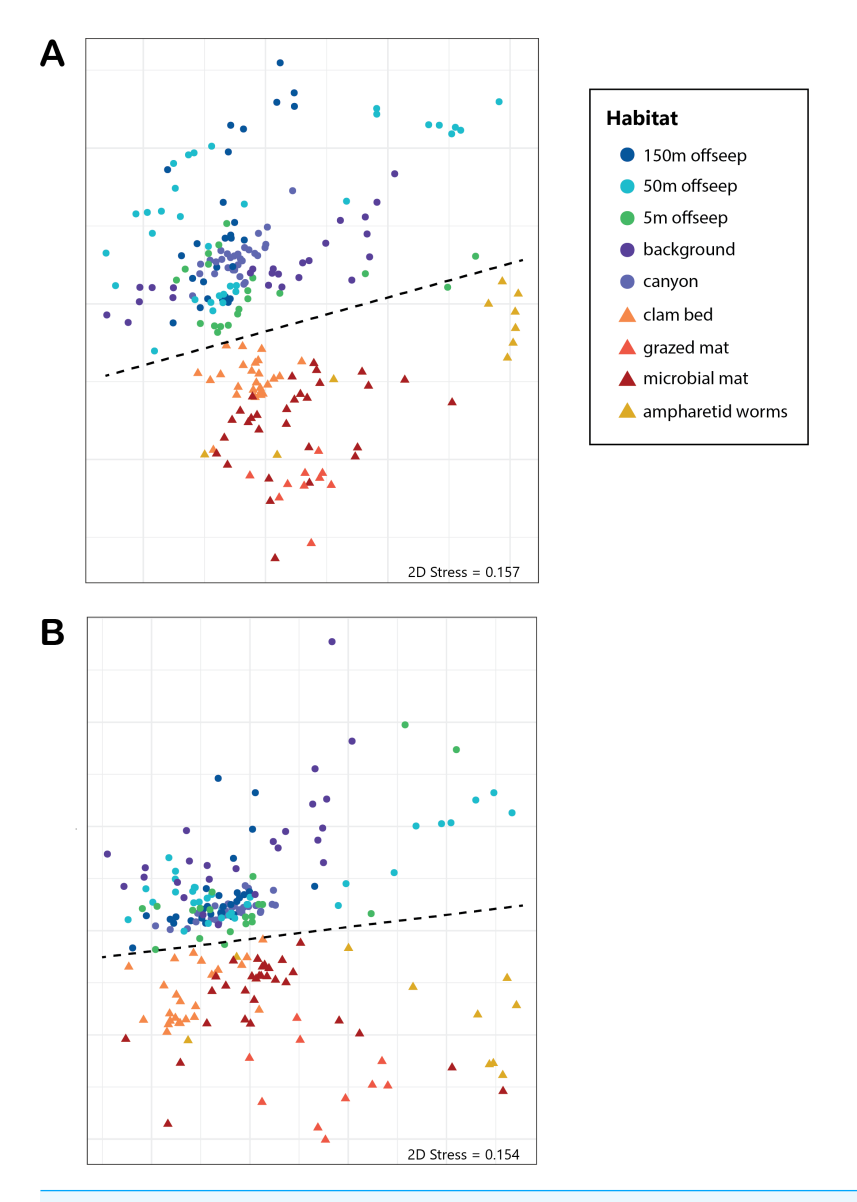


Figure 2 NMDS of microbial diversity and PICRUSt2 functional diversity. nMDS plots using Bray-Curtis distance of (A) overall microbial diversity, and (B) PICRUSt2-predicted functional diversity of a selected database of genes. This database consists of genes for methane, sulfur, and nitrogen metabolism, as well as metal transport and chelation genes, and is outlined in Table S1. Points that are warm-colored and triangle-shaped represent samples from seep-associated sites. Points that are cool-colored and circle-shaped represent samples from non-seep-associated sites. In both plots, seep and non-seep groupings were significantly different according to PERMANOVA, as indicated by the dashed line. ((A) p > 0.001, pseudo-F = 25.43, DF = 212; (B) p > 0.001, pseudo-F = 12.77, DF = 212).

Full-size DOI: 10.7717/peerj.15119/fig-2

more abundant at Westmarch (2.2 \pm 0.8%). The family Desulfobulbaceae was present both at non-seep sites (4.1 \pm 3.5%) and seep sites (3.0 \pm 3.1%) with slightly less abundance at the latter.

Archaeal ASVs were, at maximum, 39.9% of the total microbial community at each particular site, and were more abundant at seep sites (10.4 \pm 9.4% relative abundance)

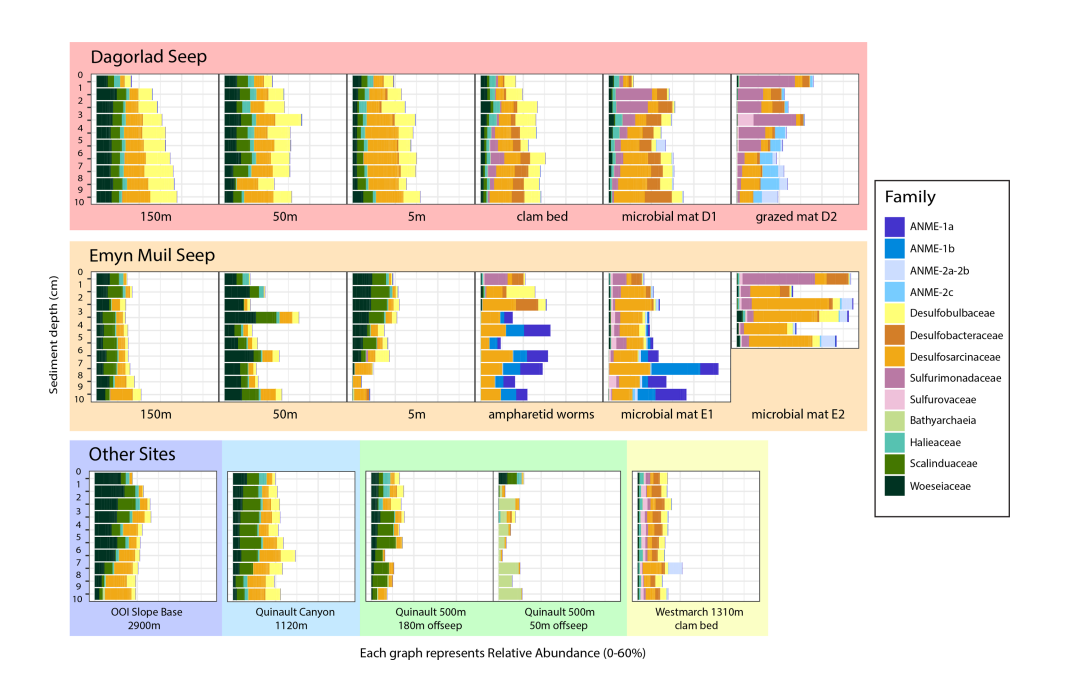


Figure 3 Taxa barplots of microbial community relative abundance of 13 most abundant families.

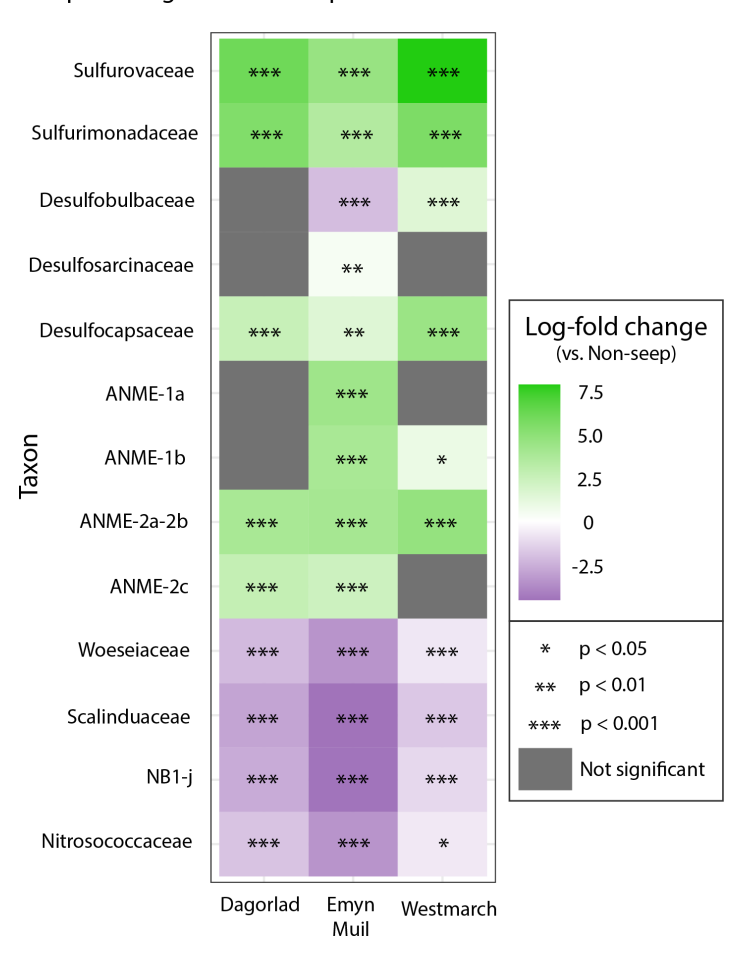
Full-size DOI: 10.7717/peerj.15119/fig-3

compared to off seeps (6.5 \pm 5.0% of the microbial community). Woesarchaeales was present at both seep and non-seep sites in about equal abundance, accounting for an average of 2.5 \pm 1.5% of the microbial community. The Archaeal family Nitrosopumilaceae made up an average of 4.2 \pm 3.6% of the total microbial community at the OOI sites, whereas it represented less than 1% of the microbial community at other sites. Similarly, 5m off-seep of Emyn Muil Seep, Asgard Archaea (Heimdallarchaeia and Lokiarchaeia) comprised 3.8 \pm 4.1% of the total community, and were less than 1% elsewhere. Additionally, at the 500m depth Quinault sample, the prominent Archaeal members were Bathyarchaeia and Hadarchaeales, averaging 3.0 \pm 3.7% and 3.1 \pm 2.2% of the total microbial community, respectively.

At seeps, ANME were prominent, and the most abundant Archaeal members of the community, making up 34.3% of Archaeal ASVs at all seep sites. The clades of ANME present varied at different seeps; ANME-2 (a, b, and c) was most abundant at Dagorlad Seep, representing 15.7% of the total microbial community at nine cm depth, whereas primarily ANME-1 (a and b) was most abundant at Emyn Muil Seep, accounting for 33.1% of the total microbial community at seven cm depth. The two clam bed samples from Westmarch Seep had ANME-2a and -2b present, but these taxa comprised at most 6.8% of the total microbial community at seven cm depth, and most samples had less than 1% of the community as ANME. ANME-2d (*Candidatus Methanoperedens* spp.) and ANME-3 were not detected in any of the samples.

Microbial and gene functional diversity

Microbial diversity, as quantified by Chao1, was highest at Quinault Canyon, averaging 1436 ± 292 (Fig. 5). The off-seep cores of Emyn Muil and Dagorlad had variable moderate



Differential Abundance of Microbial Families, Comparing Seep Sites Against Non-seep

Figure 4 ANCOM-based heatmaps of differentially abundant families between non-seep *versus* particular seep sites. Full table of log-fold changes, *p*-values, and test statistics available in Table S2.

Full-size DOI: 10.7717/peerj.15119/fig-4

to high values of diversity, with a mean of 772 \pm 404. On-seep cores had low diversity values, with a mean of 452 \pm 204. There were local peaks in diversity at the 5m off-seep sites, with values of 861 \pm 162 at this distance compared to 468 \pm 199 at the adjacent distances. The OOI sample (2,900 m non-seep) had consistent low diversity values of 510 \pm 53.

Predictive gene analysis resolved unique functions among the various habitats sampled. Off-seep samples were characterized by ammonia oxidation (*hao* genes) and sulfate reduction. On the other hand, on-seep samples were characterized by anaerobic methane oxidation and sulfate reduction. The sediment depths with high anaerobic methane oxidation also indicated higher abundance of nitrogen fixation genes.

Application of predictive gene function to our community data also identified clear differences between on and off seep dominant metabolism and process (Fig. 2B; PERMANOVA p > 0.001, pseudo-F = 12.77, DF = 212). Specifically, genes accounting

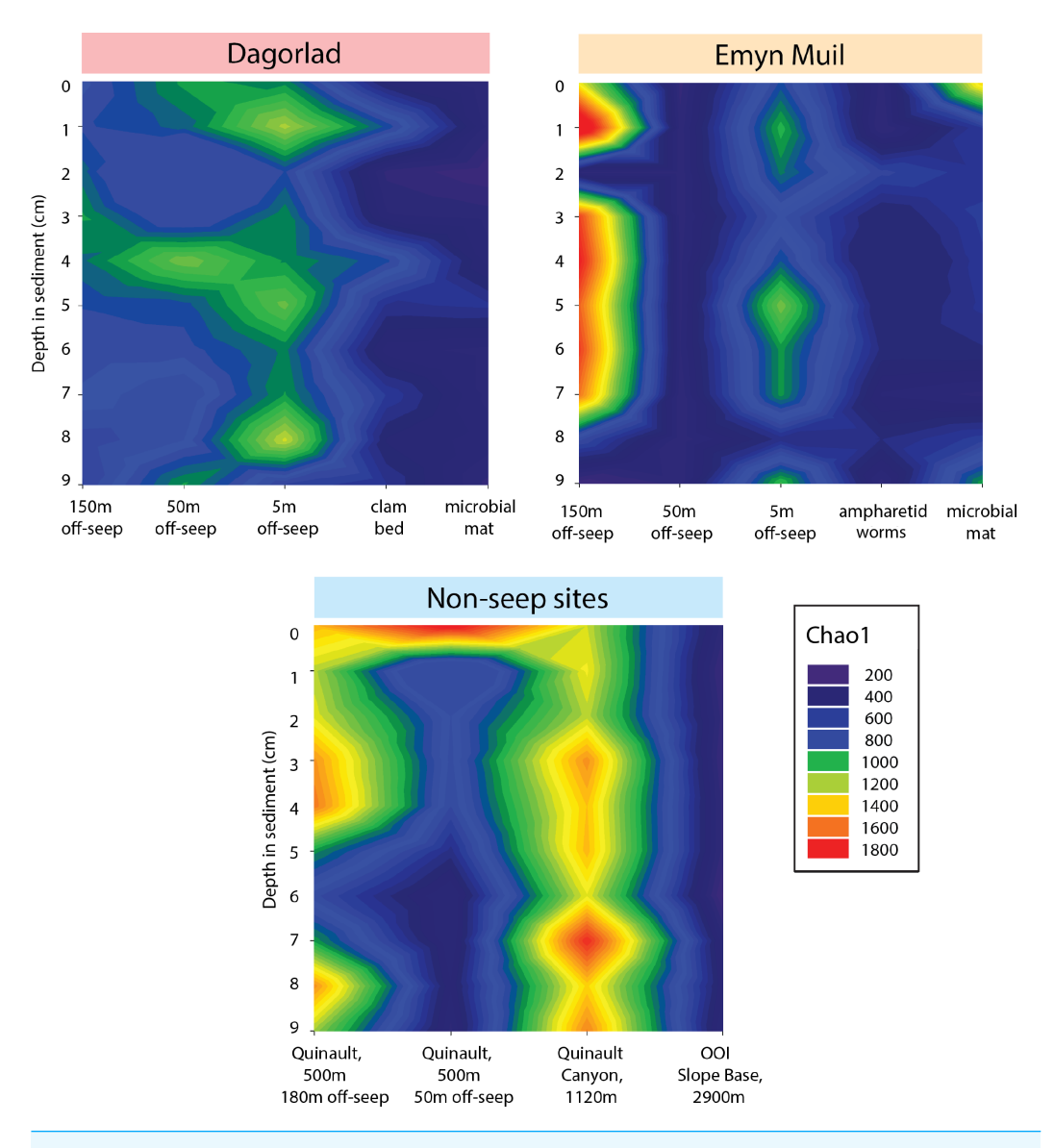


Figure 5 Chao2 diversity of Emyn Muil, Dagorlad, and non-seep sites. Heatmaps of Chao1 diversity at Dagorlad Seep, Emyn Muil Seep, and the non-seep sites. The plots represent microbial diversity within each sediment core, with surface-layer sediment at the top, and 10 cm into the sediment at the bottom. The seep heatmaps are arranged from off-seep to on-seep, left to right. The non-seep heatmap is arranged by increasing water depth left to right.

Full-size 🖴 DOI: 10.7717/peerj.15119/fig-5

for up to 20% of the variance between seep and non-seep sites included genes for handling methane, sulfate reduction, nitrification, and zinc and cobalt transport (Table 2, Table S4). Methanotrophy-related genes and sulfate reduction genes were more abundant within seep samples. Additional genes (accounting for up to 40% of the variance) included other metal transport (iron, nickel, molybdenum, and tungsten).

Predicted gene function corresponded with the geochemistry within the sediment (Fig. 6). High sulfide and methane concentrations, as well as methane oxidation genes,

Table 2 SIMPER analysis of genes contributing to up to 20% of variance between seep vs. nonseep sites.						
КО	Cumulative % variance	Process	More abundant in	Gene		
accounting for up to 20% of variance:						
K03388	5.87%	methanotrophy	Seep	hdrA2; heterodisulfide reductase subunit 2		
K03389	8.27%	methanotrophy	Seep	hdrB2; heterodisulfide reductase subunit 2		
K11261	10.61%	methanotrophy	Seep	fwdE,fmdE; formylmethanofuran dehydrogenase subunit E		
K10535	12.89%	nitrification	Non-seep	hao; hydroxylamine dehydrogenase		
K05601	15.06%	nitrification	Non-seep	hcp; hydroxylamine reductase		
K09815	16.79%	zinc transport	Seep	znuA; zinc transport system substrate-binding protein		
K03390	18.49%	methanotrophy	Seep	hdrC2; heterodisulfide reductase subunit C2		
K02190	20.10%	cobalt transport	Seep	cbiT; cobalt-precorrin-6B(C15)-methyltransferase		

appeared at seep-specific sites. However, these were variable between each on-seep sample from Dagorlad and Emyn Muil. Both Emyn Muil on-seep samples and one Dagorlad on-seep sample had high concentrations of sulfide throughout the core, increasing slightly with depth. The second Dagorlad on-seep (clam bed) sample had low sulfide at the surface and displayed a sharp increase in sulfide from 3 cm, with a peak below 5 cm depth. In the Dagorlad on-seep microbial mat sample, methane oxidation genes began to appear at 3 cm depth, although these genes were not as abundant overall as in the Emyn Muil cores, and methane concentrations were consistently high throughout this core. Both Emyn Muil on-seep cores had peaks in abundance of methane oxidation genes lower in the sediment, at 7 cm in the ampharetid sediment sample, and 4–5 cm in the microbial mat sample.

Sulfate and sulfate reduction genes were common at all sites. Sulfate concentrations were consistently around 1 micromolar off-seep and in the Dagorlad on-seep clambed sample, in which sulfate reduction genes increased with sediment core depth, and methane oxidation genes were not detectable. Sulfate concentration decreased as low as 0.01 micromolar in both on-seep samples from Emyn Muil and the on-seep microbial mat sample from Dagorlad, in which a pattern of decreasing sulfate concentration below 3 cm is mirrored by an increase in sulfate reduction genes.

DISCUSSION

Off-seep samples and depth

Between all the core samples, the microbial community showed variation based on water depth, distance from seep, and site (especially Emyn Muil *versus* Dagorlad; Fig. 2). Non-seep sites had many community members in common, such as Desulfobulbaceae, Desulfosarcinaceae, Scalinduaceae, and Woeseiaceae, and tended to cluster together on nMDS plots. However, community composition at non-seep sites displayed some variation with depth of the sites. For instance, the shallowest site (Quinault, at 500m depth) showed smaller numbers of the sulfate-reducing bacteria Desulfobulbaceae and Desulfosarcinaceae than non-seep sites at depths 1,000 m and below. Additionally, the 50m off-seep site at Quinault showed numbers of Bathyarchaeota not present in any other core. Although it is unclear why Bathyarchaeia were present in this sample and not others, Bathyarchaeal

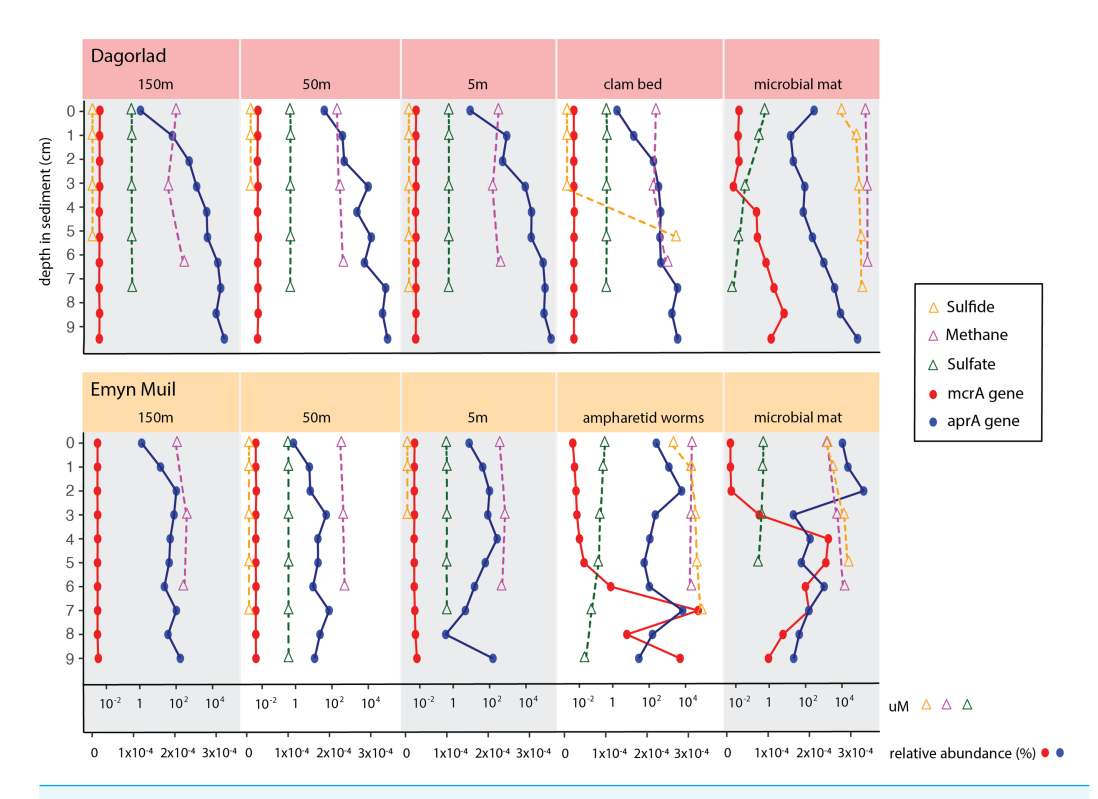


Figure 6 Comparing geochemistry values to PICRUSt2 gene abundance at seep sites.

Full-size DOI: 10.7717/peerj.15119/fig-6

genomes have been shown to contain MCR (methyl coenzyme reductase) genes, indicating that they could be conducting methanogenesis or anaerobic methane oxidation (*Evans et al.*, 2015). The OOI samples, which came from the deepest site at 2,900 m, had the lowest overall diversity of the samples, and also had greater numbers of Woeseiaceae and Nitrosopumilaceae. The samples from 2,900 m appeared to consist of a more specialized community whose members performed denitrification and ammonia oxidation. As such, these non-seep communities likely play important roles in nitrogen cycling within the deep ocean ($Mu\beta mann\ et\ al.$, 2017; $Wang\ et\ al.$, 2017).

The detection of Archaeal ASVs in all samples is limited by the choice of sequencing primer, as all primers have biases. The original F515/R805 primers (*Caporaso et al., 2011*) did not sufficiently capture many Archaeal ASVs; however, the modified F515/R805 primers (*Walters et al., 2015*), which were used for this analysis, improved detection of *Thaumarchaeota* sequences. We intentionally chose the improved F515/R805 primers for this study because they are widely used and enable easy comparison to other studies of varying habitats. However, we recognize that our data may underrepresent some Archaeal ASVs that would be better captured by other primer sets such as ArchV34 (*Fischer et al., 2016*). Focused analysis on Archaea would benefit from the use of Archaeal-specific 16S rRNA primers or an alternate technique altogether, such as metagenome analysis. See (*Fischer et al., 2016*) for further discussion of analyzing Archaea with 16S rRNA primers.

Differences between seep sites

Emyn Muil and Dagorlad Seeps, despite being in the same geographical region (35.9 km apart) and at similar depths (1,100 m and 1,000 m respectively) provided on-seep samples with distinct microbial communities. The sites varied significantly in terms of physical habitats. Dagorlad consisted of a soft sediment substrate covered by a large microbial mat that was 60m in diameter. On the other hand, Emyn Muil featured carbonate platforms that extended down into the sediment. Based on methane seep successional stages (*Bowden et al.*, 2013), this indicates that Emyn Muil is overall a much older seep that has had time to build up these extensive carbonate platforms. Thus, one likely major factor impacting the difference between the microbial communities at these two seeps is how long the methane has been seeping at each site.

The type of ANME present at the seeps varied significantly between these two locations. At Dagorlad, ANME-2a, 2b, and 2c predominate, whereas at Emyn Muil, ANME-1a and 1b are dominant. Interestingly, in terms of ANME clades and successional stages, the opposite would be expected. Typical successional patterns of microbial communities at seeps indicate that ANME-1 is an early colonizer at seeps, which is then succeeded by ANME-2, the more globally abundant ANME clade (Knittel & Boetius, 2009; Klasek et al., 2020; Thurber, Seabrook & Welsh, 2020; Knittel et al., 2005). Therefore, a different factor likely contributes to the predominance of ANME-1 at Emyn Muil. ANME-1 is the main ANME clade present in fracture-dominated sediment with high amounts of methane fluid flow (Briggs et al., 2011), or in the carbonate "chimneys" of the Black Sea (Wegener et al., 2016). Therefore, it is likely that ANME-1 remained dominant in the Emyn Muil community due to the habitat provided by the extensive carbonate structures. Previous work from our group in the Cascadia Margin region also showed varying abundances of ANME-1 and ANME-2 at different sites (Seabrook et al., 2018), although in these samples, a single ANME group (1 or 2) dominated at each specific site, rather than a mix of both as we observed at Dagorlad.

Of the sulfate-reducing bacterial partners at Dagorlad and Emyn Muil, the family Desulfosarcinaceae (containing SEEP-SRB1) appeared to be the most common and was especially abundant at Emyn Muil. SEEP-SRB2 (of the Dissulfuribacteraceae family) was generally absent, or present in abundances of 1% or lower. Desulfocapsaceae/SEEP-SRB4 was not common in the samples, yet appeared at the surface of the ampharetid bed sediment sample from Emyn Muil and within the clam bed sediment sample from Dagorlad. Some research on SEEP-SRB1 has focused on its associations with ANME-2, especially regarding methods for extracellular electron transfer with the ANME partner (*McGlynn et al.*, 2015; *Wegener et al.*, 2016; *Skennerton et al.*, 2017; *Petro et al.*, 2019). Contrarily, in our samples, SEEP-SRB1 appeared at Emyn Muil where ANME-1 was most abundant. We were unable to visualize the AOM (anaerobic oxidation of methane) aggregates *in situ*, and so the specific micro-scale associations between particular ANME and SRBs elude this analysis. Nevertheless, this research implies that different combinations of ANME and SRB associates may exist within the Cascadia Margin region.

The seep site at Westmarch cannot be compared as extensively as Emyn Muil and Dagorlad because there was only a single habitat sampled (clam bed), although we can still

compare the on-seep samples of all three seep sites. While ANME were much less abundant at Westmarch Seep, in general, there was a distinct community below seven cm depth that included ANME-2a and -2b. The appearance of ANME-2a and -2b deeper in the core could suggest bioturbation by the clams, which would oxidize the sediment deeper, depressing the sulfate methane transition zone and the depth of methane oxidation. Westmarch Seep also had consistent Sulfurovaceae throughout the cores, in contrast to Dagorlad or Emyn Muil, where Sulfurovaceae was either not present or present at one or two core depths. Interestingly, though Desulfocapsaceae/SEEP-SRB4 was not common across all samples, it appeared in the Westmarch Seep samples. As discussed above, the cores from Dagorlad and Emyn Muil that contained SEEP-SRB4 were faunal habitat sediment samples. In general, when SEEP-SRB4 appears at methane seeps, it is uncommon but most often associated with ANME-2 or -3 rather than ANME-1 (Ruff et al., 2015; Li, Yang & Zhou, 2020). However, SEEP-SRB4 can appear without ANME partners at areas with larger hydrocarbons present such as mud volcanoes, and it is suggested that this group plays a role in the degradation of larger hydrocarbons (*Kleindienst et al.*, 2012; *Petro et al.*, 2019). At Westmarch Seep, SEEP-SRB4 and ANME-2 indeed co-occur, but this trend was not consistent at the other seeps. However, across all of our seep samples, the more common pattern is the appearance of SEEP-SRB4 in seep-associated faunal sediments; perhaps there is an unexplored link here between SEEP-SRB4, seep-associated fauna, and type of hydrocarbon fueling the seep. While we did not expect to find any longer chain hydrocarbons beyond methane, we also did not specifically quantify it.

"Transitional" samples and the methane seep sphere of influence

The "marginal" seep samples of ampharetid worm beds and vesicomyid clam beds, as well as the 5m off-seep samples, show some interesting patterns in microbial communities and diversity that indicate a transition between non-seep and seep habitats. The ampharetid worm bed core from Emyn Muil overall grouped with other seep-associated samples, and also formed a smaller grouping, as seen to the bottom-right side of the nMDS plots (yellow triangle symbols, Fig. 2). ANME-1 was clearly present deeper in this sample, but there were few Sulfurimonadaceae present in core depths below one cm, unlike all other seep sites. The ampharetid bed samples thus appeared to have a microbial community capable of seep-associated anaerobic oxidation of methane, but different from other seep-associated samples. Samples from the Dagorlad clam bed core (orange triangle symbols, Fig. 2), clustered with other seep-associated samples but were closer in community composition to non-seep samples than to other seep samples. This pattern appears to be mirrored by the 5m off-seep samples within the nMDS plots (green circle symbols, Fig. 2). The 5 m samples clustered overall with non-seep samples but were generally closer in composition to the seep-associated samples. Of note, these patterns apply both in terms of microbial community composition, as well as targeted metabolic similarity of the PICRUSt2 database. That is to say, the 5m off-seep samples and the clambed samples also had similar metabolic profiles in terms of sulfur, nitrogen, and methane metabolism, and metal transport. With regard to diversity, the 5m off-seep samples also showed local maxima in diversity values, positioning them between seep and non-seep in terms of community members and metabolisms. This observation illustrates that there is a gradient of community composition and metabolism moving from on-seep to off-seep that increases local microbial diversity.

The patterns in microbial diversity tended to follow expected patterns of faunal diversity. Previous patterns in macrofaunal diversity also exhibit similar trends moving from on-to off-seep, where the zones of transition between seep and non-seep contained both seependemic as well as non-seep-specialized organisms, increasing overall species diversity (*Levin et al.*, 2010). Intermediate habitats that transition between different specialized habitats tend to have higher diversity of fauna. For example, submarine canyons host highly heterogeneous marine habitats, and frequently have a large amount of faunal diversity (*Ramirez-Llodra et al.*, 2010; *De Leo & Puig*, 2018). It is important to note that all of our samples from this study came from within canyons, and that, these samples showed some of the greatest diversity values amongst all seep samples we have collected (*Seabrook et al.*, 2018; *Thurber*, *Seabrook & Welsh*, 2020). Within these canyon-specific samples, microbial diversity and faunal diversity appear to be related, indicating that the unique ecosystems of methane seeps impact surrounding areas in terms of both microbial and faunal diversity (*Levin et al.*, 2016).

Biogeochemistry and metabolic analysis

Application of combined gene prediction and biogeochemistry elucidated some clear patterns within these briefly visited seeps. Predicted gene abundances showed that sulfate reducing and sulfide oxidizing genes predominated at shallower core depths, and methane oxidizing genes predominated at deeper core depths. Unsurprisingly, predicted anaerobic methane oxidizing genes increased where the sediment sulfate concentrations began to drop, indicative of a sulfate-methane transition zone (*Ruff et al.*, 2015).

Seep samples had higher relative abundance predictions of zinc, cobalt, nickel, and tungsten-handling proteins, and these contributed to major differences in the predicted gene composition between seep and non-seep samples (Table 2, Table S4). Nickel and zinc are needed for key proteins involved in methanotrophy (Glass & Orphan, 2012), and so acquisition of these metals is particularly important to ANME at seeps. Cobalt and tungsten are necessary for enzymes involved in core metabolism, but often precipitate in sulfidic seep sediment and are less bioavailable (Glass et al., 2014). Therefore, on-seep microbes logically need to prioritize acquisition of what little cobalt and tungsten are available. Thus, our data reflect biogeochemical trends in metal availability particular to methane seep systems.

Application of predictive gene pipelines was surprisingly informative for methane seeps. Although gene abundances were not directly measured in our analysis, and instead estimated based on 16S rRNA gene data using the PICRUSt2 pipeline, the correspondence between the measured geochemical values and the PICRUSt2 genes indicates that this analytical approach is useful even in deep-sea chemosynthetic ecosystems. Additionally, the PICRUSt2 analysis can reflect genuine trends in metabolism by summarizing genes of particular interest across whole communities. We found PICRUSt2 analysis useful for summarizing the metabolic potential of different microbial communities and revealing the transition of seep-associated metabolisms to non-seep-associated metabolisms.

CONCLUSIONS

This work focused on the microbial communities of methane seeps from geographically close sites in the Northeastern Pacific Ocean. The microbial communities distant from methane seeps were distinct in both diversity and metabolic capability from on-seep microbial communities. The communities between methane seeps and off-seep sites indicated that the microbial influence of seeps extends outwards and creates transitional communities, or ecotones of community overlap. Off-seep communities differed from each other based on depth, whereas on-seep communities differed from each other based on gross seep morphology, which indicated the seep succession state and age were likely deterministic of the microbial community composition. Finally, applying predictive gene pipelines to these samples was highly informative, indicating transitions in metabolic capability from off-seep to on-seep. Overall, methane seeps contribute to both local-scale ocean habitats and the global carbon budget, and this work demonstrates how the microbial communities at seeps factor into these broader systems with a sphere of influence on biodiversity that extends beyond the seep habitats themselves.

ADDITIONAL INFORMATION AND DECLARATIONS

Funding

This research was funded by NOAA Ocean Exploration Grant NA19OAR0110301 and NSF Grants 2046800 and 1933165. The funders had no role in study design, data collection and analysis, decision to publish, or preparation of the manuscript.

Grant Disclosures

The following grant information was disclosed by the authors:

NOAA Ocean Exploration Grant: NA19OAR0110301.

NSF Grants: 2046800, 1933165.

Competing Interests

The authors declare there are no competing interests.

Author Contributions

- Susie Cummings conceived and designed the experiments, performed the experiments, analyzed the data, prepared figures and/or tables, authored or reviewed drafts of the article, and approved the final draft.
- Lila M. Ardor Bellucci performed the experiments, analyzed the data, prepared figures and/or tables, authored or reviewed drafts of the article, and approved the final draft.
- Sarah Seabrook conceived and designed the experiments, analyzed the data, authored or reviewed drafts of the article, and approved the final draft.
- Nicole A. Raineault performed the experiments, authored or reviewed drafts of the article, and approved the final draft.
- Kerry L. McPhail analyzed the data, authored or reviewed drafts of the article, and approved the final draft.

• Andrew R. Thurber conceived and designed the experiments, performed the experiments, analyzed the data, authored or reviewed drafts of the article, and approved the final draft.

Field Study Permissions

The following information was supplied relating to field study approvals (i.e., approving body and any reference numbers):

Ocean Exploration Trust: E/V Nautilus expedition NA121.

DNA Deposition

The following information was supplied regarding the deposition of DNA sequences: The full 16S rRNA gene data is available in the NCBI Sequence Read Archive: PRJNA718843.

Data Availability

The following information was supplied regarding data availability:

The full pipelines for QIIME2 and PICRUSt2 analyses are available in the Supplementary
File.

Supplemental Information

Supplemental information for this article can be found online at http://dx.doi.org/10.7717/peerj.15119#supplemental-information.

REFERENCES

- Beal EJ, House CH, Orphan VJ. 2009. Manganese- and iron-dependent marine methane oxidation. *Science* 325(5937):184–187 DOI 10.1126/science.1169984.
- Berger S, Cabrera-Orefice A, Jetten MSM, Brandt U, Welte CU. 2021. Investigation of central energy metabolism-related protein complexes of ANME-2d methan-otrophic archaea by complexome profiling. *Biochimica Et Biophysica Acta (BBA)—Bioenergetics* 1862(1):148308 DOI 10.1016/j.bbabio.2020.148308.
- Bhattarai S, Cassarini C, Gonzalez-Gil G, Egger M, Slomp CP, Zhang Y, Esposito G, Lens PNL. 2017. Anaerobic methane-oxidizing microbial community in a coastal marine sediment: anaerobic methanotrophy dominated by ANME-3. *Microbial Ecology* 74(3):608–622 DOI 10.1007/s00248-017-0978-y.
- Boetius A, Ravenschlag K, Schubert CJ, Rickert D, Widdel F, Gieseke A, Amann R, Jørgensen BB, Witte U, Pfannkuche O. 2000. A marine microbial consortium apparently mediating anaerobic oxidation of methane. *Nature* 407(6804):6804 DOI 10.1038/35036572.
- **Boetius A, Suess E. 2004.** Hydrate Ridge: A natural laboratory for the study of microbial life fueled by methane from near-surface gas hydrates. *Chemical Geology* **205(3)**:291–310 DOI 10.1016/j.chemgeo.2003.12.034.
- Bolyen E, Rideout JR, Dillon MR, Bokulich NA, Abnet CC, Al-Ghalith GA, Alexander H, Alm EJ, Arumugam M, Asnicar F, Bai Y, Bisanz JE, Bittinger K, Brejnrod A, Brislawn CJ, Brown CT, Callahan BJ, Caraballo-Rodríguez AM, Chase

- **J, Caporaso JG. 2019.** Reproducible, interactive, scalable and extensible microbiome data science using QIIME 2. *Nature Biotechnology* **37(8)**:852–857 DOI 10.1038/s41587-019-0209-9.
- Bowden DA, Rowden AA, Thurber AR, Baco AR, Levin LA, Smith CR. 2013. Cold seep epifaunal communities on the Hikurangi margin, New Zealand: composition, succession, and vulnerability to human activities. *PLOS ONE* **8**(10):e76869 DOI 10.1371/journal.pone.0076869.
- Briggs BR, Pohlman JW, Torres M, Riedel M, Brodie EL, Colwell FS. 2011. Macroscopic biofilms in fracture-dominated sediment that anaerobically oxidize methane. *Applied and Environmental Microbiology* 77(19):6780–6787 DOI 10.1128/AEM.00288-11.
- **De Leo CF, Puig P. 2018.** Bridging the gap between the shallow and deep oceans: the key role of submarine canyons. *Progress in Oceanography* **169**:1–5 DOI 10.1016/j.pocean.2018.08.006.
- Caporaso JG, Lauber CL, Walters WA, Berg-Lyons D, Lozupone CA, Turnbaugh PJ, Fierer N, Knight R. 2011. Global patterns of 16S rRNA diversity at a depth of millions of sequences per sample. *Proceedings of the National Academy of Sciences of the United States of America* 108(supplement_1):4516–4522 DOI 10.1073/pnas.1000080107.
- Cline JD. 1969. Spectrophotometric determination of hydrogen sulfide in natural waters. *Limnology and Oceanography* 14:454–458 DOI 10.4319/lo.1969.14.3.0454.
- **Dekas AE, Chadwick GL, Bowles MW, Joye SB, Orphan VJ. 2014.** Spatial distribution of nitrogen fixation in methane seep sediment and the role of the ANME archaea. *Environmental Microbiology* **16(10)**:3012–3029 DOI 10.1111/1462-2920.12247.
- Dekas AE, Fike DA, Chadwick GL, Green-Saxena A, Fortney J, Connon SA, Dawson KS, Orphan VJ. 2018. Widespread nitrogen fixation in sediments from diverse deepsea sites of elevated carbon loading. *Environmental Microbiology* 20(12):4281–4296 DOI 10.1111/1462-2920.14342.
- Douglas GM, Maffei VJ, Zaneveld JR, Yurgel SN, Brown JR, Taylor CM, Huttenhower C, Langille MGI. 2020. PICRUSt2 for prediction of metagenome functions. *Nature Biotechnology* 38(6):685–688 DOI 10.1038/s41587-020-0548-6.
- Evans PN, Parks DH, Chadwick GL, Robbins SJ, Orphan VJ, Golding SD, Tyson GW. 2015. Methane metabolism in the archaeal phylum Bathyarchaeota revealed by genome-centric metagenomics. *Science* 350(6259):434–438

 DOI 10.1126/science.aac7745.
- Felden J, Ruff SE, Ertefai T, Inagaki F, Hinrichs K-U, Wenzhöfer F. 2014. Anaerobic methanotrophic community of a 5346-m-deep vesicomyid clam colony in the Japan Trench. *Geobiology* 12(3):183–199 DOI 10.1111/gbi.12078.
- **Gillard B, Chatzievangelou D, Thomsen L, Ullrich MS. 2019.** Heavy-metal-resistant microorganisms in deep-sea sediments disturbed by mining activity: an application toward the development of experimental in vitro systems. *Frontiers in Marine Science* **6**:462 DOI 10.3389/fmars.2019.00462.

- **Glass J, Orphan V. 2012.** Trace metal requirements for microbial enzymes involved in the production and consumption of methane and nitrous oxide. *Frontiers in Microbiology* **3**:61 DOI 10.3389/fmicb.2012.00061.
- Glass JB, Yu H, Steele JA, Dawson KS, Sun S, Chourey K, Pan C, Hettich RL, Orphan VJ. 2014. Geochemical, metagenomic and metaproteomic insights into trace metal utilization by methane-oxidizing microbial consortia in sulphidic marine sediments. *Environmental Microbiology* 16(6):1592–1611 DOI 10.1111/1462-2920.12314.
- **Guillon E, Menot L, Decker C, Krylova E, Olu K. 2017.** The vesicomyid bivalve habitat at cold seeps supports heterogeneous and dynamic macrofaunal assemblages. *Deep Sea Research Part I: Oceanographic Research Papers* **120**:1–13 DOI 10.1016/j.dsr.2016.12.008.
- **Fischer MA, Güllert S, Neulinger SC, Streit WR, Schmitz RA. 2016.** Evaluation of 16S rRNA gene primer pairs for monitoring microbial community structures showed high reproducibility within and low comparability between datasets generated with multiple archaeal and bacterial primer pairs. *Frontiers in Microbiology* 7:1297 DOI 10.3389/fmicb.2016.01297.
- Haroon MF, Hu S, Shi Y, Imelfort M, Keller J, Hugenholtz P, Yuan Z, Tyson GW. 2013. Anaerobic oxidation of methane coupled to nitrate reduction in a novel archaeal lineage. *Nature* 500(7464):567–570 DOI 10.1038/nature12375.
- Joseph C, Campbell KA, Torres ME, Martin RA, Pohlman JW, Riedel M, Rose K. 2013. Methane-derived authigenic carbonates from modern and paleoseeps on the Cascadia margin: Mechanisms of formation and diagenetic signals. *Palaeogeography, Palaeoclimatology, Palaeoecology* 390:52–67 DOI 10.1016/j.palaeo.2013.01.012.
- **Kapili BJ, Barnett SE, Buckley DH, Dekas AE. 2020.** Evidence for phylogenetically and catabolically diverse active diazotrophs in deep-sea sediment. *The ISME Journal* **14(4)**:971–983 DOI 10.1038/s41396-019-0584-8.
- Klasek S, Torres ME, Bartlett DH, Tyler M, Hong W-L, Colwell F. 2020. Microbial communities from Arctic marine sediments respond slowly to methane addition during ex situ enrichments. *Environmental Microbiology* 22(5):1829–1846 DOI 10.1111/1462-2920.14895.
- Kleindienst S, Ramette A, Amann R, Knittel K. 2012. Distribution and in situ abundance of sulfate-reducing bacteria in diverse marine hydrocarbon seep sediments. *Environmental Microbiology* **14(10)**:2689–2710 DOI 10.1111/j.1462-2920.2012.02832.x.
- **Knittel K, Boetius A. 2009.** Anaerobic oxidation of methane: progress with an unknown process. *Annual Review of Microbiology* **63**(1):311–334 DOI 10.1146/annurey.micro.61.080706.093130.
- Knittel K, Lösekann T, Boetius A, Kort R, Amann R. 2005. Diversity and distribution of methanotrophic archaea at cold seeps. *Applied and Environmental Microbiology* 71(1):467–479 DOI 10.1128/AEM.71.1.467-479.2005.
- **Kvenvolden KA. 1988.** Methane hydrate—a major reservoir of carbon in the shallow geosphere? *Chemical Geology* **71(1)**:41–51 DOI 10.1016/0009-2541(88)90104-0.

- Lahti L, Shetty S, Turaga N, Leung E, Gilmore R, Salojärvi J, Blake T, Obenchain V, Ramos M, Pagès H, Fan H, Salosensaari A. 2017. Tools for microbiome analysis in R. Version 3.16. *Available at https://microbiome.github.io/tutorials/*.
- Leu AO, Cai C, McIlroy SJ, Southam G, Orphan VJ, Yuan Z, Hu S, Tyson GW. 2020. Anaerobic methane oxidation coupled to manganese reduction by members of the Methanoperedenaceae. *The ISME Journal* 14(4):1030–1041 DOI 10.1038/s41396-020-0590-x.
- Levin LA, Baco AR, Bowden DA, Colaco A, Cordes EE, Cunha MR, Demopoulos AWJ, Gobin J, Grupe BM, Le J, Metaxas A, Netburn AN, Rouse GW, Thurber AR, Tunnicliffe V, Van Dover CL, Vanreusel A, Watling L. 2016. Hydrothermal vents and methane seeps: rethinking the sphere of influence. *Frontiers in Marine Science* 3:72 DOI 10.3389/fmars.2016.00072.
- **Levin LA, Mendoza GF, Gonzalez JP, Thurber AR, Cordes EE. 2010.** Diversity of bathyal macrofauna on the northeastern Pacific margin: the influence of methane seeps and oxygen minimum zones. *Marine Ecology* **31(1)**:94–110 DOI 10.1111/j.1439-0485.2009.00335.x.
- **Levin LA, Sibuet M. 2012.** Understanding continental margin biodiversity: a new imperative. *Annual Review of Marine Science* **4(1)**:79–112

 DOI 10.1146/annurev-marine-120709-142714.
- Levin LA, Ziebis W, Mendoza G, Growney V, Tryon M, Brown K, Mahn C, Gieskes J, Rathburn A. 2003. Spatial heterogeneity of macrofauna at northern California methane seeps: influence of sulfide concentration and fluid flow. *Marine Ecology Progress Series* 265:123–139 DOI 10.3354/meps265123.
- **Li H, Yang Q, Zhou H. 2020.** Niche differentiation of sulfate- and iron-dependent anaerobic methane oxidation and methylotrophic methanogenesis in deep sea methane seeps. *Frontiers in Microbiology* **11**:1409 DOI 10.3389/fmicb.2020.01409.
- **Lin H, Peddada SD. 2020.** Analysis of compositions of microbiomes with bias correction. *Nature Communications* **11(1)**:Article 1 DOI 10.1038/s41467-020-17041-7.
- **Luff R, Wallmann K. 2003.** Fluid flow, methane fluxes, carbonate precipitation and biogeochemical turnover in gas hydrate-bearing sediments at Hydrate Ridge, Cascadia Margin: numerical modeling and mass balances. *Geochimica et Cosmochimica Acta* **67(18)**:3403–3421 DOI 10.1016/S0016-7037(03)00127-3.
- McGlynn SE, Chadwick GL, Kempes CP, Orphan VJ. 2015. Single cell activity reveals direct electron transfer in methanotrophic consortia. *Nature* 526(7574):531–535 DOI 10.1038/nature15512.
- **McMurdie PJ, Holmes S. 2013.** phyloseq: an R package for reproducible interactive analysis and graphics of microbiome census data. *PLOS ONE* **8(4)**:e61217 DOI 10.1371/journal.pone.0061217.
- Merle SG, Embley RW, Johnson HP, Lau T-K, Phrampus BJ, Raineault NA, Gee LJ. 2021. Distribution of methane plumes on cascadia margin and implications for the landward limit of methane hydrate stability. *Frontiers in Earth Science* 9:531714 DOI 10.3389/feart.2021.531714.

- Mußmann M, Pjevac P, Krüger K, Dyksma S. 2017. Genomic repertoire of the Woeseiaceae/JTB255, cosmopolitan and abundant core members of microbial communities in marine sediments. *The ISME Journal* 11(5):1276–1281 DOI 10.1038/ismej.2016.185.
- Niemann H, Fischer D, Graffe D, Knittel K, Montiel A, Heilmayer O, Nöthen K, Pape T, Kasten S, Bohrmann G, Boetius A, Gutt J. 2009. Biogeochemistry of a low-activity cold seep in the Larsen B area, western Weddell Sea, Antarctica. *Biogeosciences* 6(11):2383–2395 DOI 10.5194/bg-6-2383-2009.
- Oksanen J, Guillaume Blanchet F, Friendly M, Kindt R, Legendre P, McGlinn D, Minchin PR, O'Hara RB, Simpson GL, Solymos P, Stevens MHH, Szoecs E, Wagner H. 2020. vegan: community ecology package. R package version 2.5-7. Available at https://CRAN.R-project.org/package=vegan.
- Orphan VJ, House CH, Hinrichs K-U, McKeegan KD, De Long EF. 2002. Multiple archaeal groups mediate methane oxidation in anoxic cold seep sediments. *Proceedings of the National Academy of Sciences of the United States of America* 99(11):7663–7668 DOI 10.1073/pnas.072210299.
- Pachiadaki MG, Sintes E, Bergauer K, Brown JM, Record NR, Swan BK, Mathyer ME, Hallam SJ, Lopez-Garcia P, Takaki Y, Nunoura T, Woyke T, Herndl GJ, Stepanauskas R. 2017. Major role of nitrite-oxidizing bacteria in dark ocean carbon fixation. *Science* 358(6366):1046–1051 DOI 10.1126/science.aan8260.
- Petro C, Jochum LM, Schreiber L, Marshall IPG, Schramm A, Kjeldsen KU. 2019. Single-cell amplified genomes of two uncultivated members of the deltaproteobacterial SEEP-SRB1 clade, isolated from marine sediment. *Marine Genomics* **46**:66–69 DOI 10.1016/j.margen.2019.01.004.
- Ramirez-Llodra E, Brandt A, Danovaro R, De Mol B, Escobar E, German CR, Levin LA, Martinez Arbizu P, Menot L, Buhl-Mortensen P, Narayanaswamy BE, Smith CR, Tittensor DP, Tyler PA, Vanreusel A, Vecchione M. 2010. Deep, diverse and definitely different: Unique attributes of the world's largest ecosystem. *Biogeosciences* 7(9):2851–2899 DOI 10.5194/bg-7-2851-2010.
- **Reeburgh WS. 2007.** Oceanic methane biogeochemistry. *Chemical Reviews* **107(2)**:486–513 DOI 10.1021/cr050362v.
- Ruff SE, Biddle JF, Teske AP, Knittel K, Boetius A, Ramette A. 2015. Global dispersion and local diversification of the methane seep microbiome. *Proceedings of the National Academy of Sciences of the United States of America* 112(13):4015–4020 DOI 10.1073/pnas.1421865112.
- Ruff SE, Felden J, Gruber-Vodicka HR, Marcon Y, Knittel K, Ramette A, Boetius A. **2019.** In situ development of a methanotrophic microbiome in deep-sea sediments. *The ISME Journal* **13(1)**:Article 1 DOI 10.1038/s41396-018-0263-1.
- **Ruppel CD, Kessler JD. 2017.** The interaction of climate change and methane hydrates. *Reviews of Geophysics* **55(1)**:126–168 DOI 10.1002/2016RG000534.
- Sahling H, Galkin SV, Salyuk A, Greinert J, Foerstel H, Piepenburg D, Suess E. 2003. Depth-related structure and ecological significance of cold-seep communities—a

- case study from the Sea of Okhotsk. *Deep Sea Research Part I: Oceanographic Research Papers* **50(12)**:1391–1409 DOI 10.1016/j.dsr.2003.08.004.
- Seabrook S, De Leo CF, Baumberger T, Raineault N, Thurber AR. 2018. Heterogeneity of methane seep biomes in the Northeast Pacific. *Deep Sea Research Part II: Topical Studies in Oceanography* **150**:195–209 DOI 10.1016/j.dsr2.2017.10.016.
- **Seabrook S, De Leo FC, Thurber AR. 2019.** Flipping for food: the use of a methane seep by Tanner Crabs (Chionoecetes tanneri). *Frontiers in Marine Science* **6**:43 DOI 10.3389/fmars.2019.00043.
- Skennerton CT, Chourey K, Iyer R, Hettich RL, Tyson GW, Orphan VJ. 2017. Methane-fueled syntrophy through extracellular electron transfer: uncovering the genomic traits conserved within diverse bacterial partners of anaerobic methanotrophic archaea. *MBio* 8(4):e00530-17 DOI 10.1128/mBio.00530-17.
- Suess E, Carson B, Ritger SD, Moore JC, Jones ML, Kulm LD, Cochrane GR. 1985.

 Biological communities at vent sites along the subduction zone off Oregon. *Bulletin of the Biological Society of Washington* **6**:475–484.
- Suter EA, Pachiadaki MG, Montes E, Edgcomb VP, Scranton MI, Taylor CD, Taylor GT. 2021. Diverse nitrogen cycling pathways across a marine oxygen gradient indicate nitrogen loss coupled to chemoautotrophic activity. *Environmental Microbiology* 23(6):2747–2764 DOI 10.1111/1462-2920.15187.
- Thurber AR, Levin LA, Orphan VJ, Marlow JJ. 2012. Archaea in metazoan diets: implications for food webs and biogeochemical cycling. *The ISME Journal* 6(8):1602–1612 DOI 10.1038/ismej.2012.16.
- Thurber AR, Levin LA, Rowden AA, Sommer S, Linke P, Kröger K. 2013. Microbes, macrofauna, and methane: a novel seep community fueled by aerobic methanotrophy. *Limnology and Oceanography* **58**(5):1640–1656 DOI 10.4319/lo.2013.58.5.1640.
- **Thurber AR, Seabrook S, Welsh RM. 2020.** Riddles in the cold: Antarctic endemism and microbial succession impact methane cycling in the Southern Ocean. *Proceedings of the Royal Society B: Biological Sciences* **287(1931)**:20201134 DOI 10.1098/rspb.2020.1134.
- Treude T, Orphan V, Knittel K, Gieseke A, House CH, Boetius A. 2007. Consumption of methane and CO2 by methanotrophic microbial mats from gas seeps of the anoxic black sea. *Applied and Environmental Microbiology* 73(7):2271–2283 DOI 10.1128/AEM.02685-06.
- Turner PJ, Ball B, Diana Z, Fariñas Bermejo A, Grace I, McVeigh D, Powers MM, Van Audenhaege L, Maslakova S, Young CM, Van Dover CL. 2020. Methane seeps on the US Atlantic Margin and their potential importance to populations of the commercially valuable deep-sea Red Crab, Chaceon quinquedens. *Frontiers in Marine Science* 7:75 DOI 10.3389/fmars.2020.00075.
- Vigneron A, Cruaud P, Pignet P, Caprais J-C, Cambon-Bonavita M-A, Godfroy A, Toffin L. 2013. Archaeal and anaerobic methane oxidizer communities in the Sonora Margin cold seeps, Guaymas Basin (Gulf of California). *The ISME Journal* 7(8):Article 8 DOI 10.1038/ismej.2013.18.

- Waite DW, Chuvochina M, Pelikan C, Parks DH, Yilmaz P, Wagner M, Loy A, Naganuma T, Nakai R, Whitman WB, Hahn MW, Kuever J, Hugenholtz P. 2020. Proposal to reclassify the proteobacterial classes Deltaproteobacteria and Oligoflexia, and the phylum Thermodesulfobacteria into four phyla reflecting major functional capabilities. *International Journal of Systematic and Evolutionary Microbiology* 70(11):5972–6016 DOI 10.1099/ijsem.0.004213.
- Wallmann K, Linke P, Suess E, Bohrmann G, Sahling H, Schlüter M, Dählmann A, Lammers S, Greinert J, von Mirbach N. 1997. Quantifying fluid flow, solute mixing, and biogeochemical turnover at cold vents of the eastern Aleutian subduction zone. *Geochimica et Cosmochimica Acta* 61(24):5209–5219 DOI 10.1016/S0016-7037(97)00306-2.
- Walters W, Hyde ER, Berg-Lyons D, Ackermann G, Humphrey G, Parada A, Gilbert JA, Jansson JK, Caporaso JG, Fuhrman JA, Apprill A, Knight R. 2015. Improved bacterial 16S rRNA gene (V4 and V4-5) and Fungal internal transcribed spacer marker gene primers for microbial community surveys. *MSystems* 1(1):e00009–15 DOI 10.1128/mSystems.00009-15.
- Wang J, Kan J, Zhang X, Xia Z, Zhang X, Qian G, Miao Y, Leng X, Sun J. 2017. Archaea dominate the ammonia-oxidizing community in deep-sea sediments of the Eastern Indian Ocean—from the equator to the Bay of Bengal. *Frontiers in Microbiology* 8:415 DOI 10.3389/fmicb.2017.00415.
- Wegener G, Krukenberg V, Ruff SE, Kellermann MY, Knittel K. 2016. Metabolic capabilities of microorganisms involved in and associated with the anaerobic oxidation of methane. *Frontiers in Microbiology* 7:46 DOI 10.3389/fmicb.2016.00046.